

Processing of Mica/Epoxy Nanocomposites by Ultrasound Mixing

Amar Boukerrou,¹ Jannick Duchet,² Said Fellahi,³ Henry Sautereau²

¹Laboratoire des Matériaux Organiques, Université Abderrahmane Mira, Bejaia 06000, Algeria

²Laboratoire des Matériaux Macromoléculaires, IMP, UMR 5627, INSA de Lyon, Bâtiment Jules Verne, 20 Avenue Albert Einstein, 69621 Villeurbanne Cedex France

³Département de Génie des Polymères, Institut Algérien du Pétrole, Boumerdes 35000, Algeria

Received 13 June 2006; accepted 17 January 2007

DOI 10.1002/app.26292

Published online 23 April 2007 in Wiley InterScience (www.interscience.wiley.com).

ABSTRACT: Rubbery mica/epoxy nanocomposites are synthesized by *in situ* polymerization, and their morphology, mechanical, and viscoelastic properties were investigated by wide angle X-ray scattering (WAXS), transmission electron microscopy (TEM), tensile testing, and dynamic mechanical thermal analysis (DMTA). Ultrasonicator was used as a means of applying external shearing forces to disperse the silicate clay layers in the epoxy matrix. The first step of the nanocomposite preparation consisted of swelling the mica in a curing agent, i.e., aliphatic diamine based on polyoxypropylene backbone having a low viscosity for better diffusion into the intragalleries. Then, the epoxy prepolymer was added into the mixture. It was expected to have better dispersion and intercalation of the nanoclay in the matrix.

The study showed that the organomodification of mica with octadecylammonium ions leads to an increase in the initial *d*-spacing ($[d_{001}]$ peak) from 12.3 to 28.1 Å, determined by WAXS, indicating the occurrence of an intercalation. The addition of 5 per hundred resin (phr) of MICAC18 into the epoxy matrix resulted in finer dispersion as evidenced by both the disappearance of the diffraction peak in the WAXS pattern and TEM images. The mechanical and viscoelastic properties were improved for both MICA and MICAC18 nanocomposites, however, more pronounced for the modified ones. © 2007 Wiley Periodicals, Inc. *J Appl Polym Sci* 105: 1420–1425, 2007

Key words: mica; epoxy; nanocomposites

INTRODUCTION

Polymer-layered silicate nanocomposites have attracted a great deal of attention in both academic and industrial fields, since many potential improvements are waited by introducing a small amount of nanosize clay particles in polymers: increase of mechanical properties, improvement of barrier properties and flame retardation, and better dimensional and thermal stability.¹ Among polymers, epoxy resins find many industrial applications in adhesives, construction materials, composites, laminates, coatings, and air craft because of their high strength, low viscosity, low volatility, low shrinkage during cure, low creep, and good adhesion to many substrates.² Therefore, epoxy resins are one of the most commonly studied polymers in the preparation of nanocomposites with layered silicates, because the polar epoxy monomers can easily diffuse into the clay galleries.^{3,4} In fact, the matrix/filler type system, the extent of filler adhesion to the matrix, and the levels of dispersion of the filler throughout the matrix degree are among the parameters which highly determine any enhancement of a

particular property of nanocomposites.⁵ Moreover, the nature of the curing agent as well as the curing conditions, especially the temperature is expected to play a role in the exfoliation process.³ In this respect, Kornman et al.⁶ reported that a long chain alkylamine, having a chain of more than eight carbon atoms, could significantly result in an exfoliated clay structure. Furthermore, a balance between the intragalleries and the extragallery polymerization rates is essential to exfoliate the clay into an epoxy system.⁷ According to literature data,^{8–12} there are three different methods to synthesize polymer–clay nanocomposites: melt intercalation process for thermoplastic polymers; solution method, where both organoclay and polymer precursor are dissolved in a polar organic solvent; and *in situ* polymerization technique. The latter one was found to be the most effective technique for thermoset polymer matrix nanocomposites.⁷

On the other hand, the commonly used techniques for processing clay–epoxy nanocomposites are direct mixing and solution mixing.¹³ However, these two techniques produce intercalated or intercalated/exfoliated composites or rather fully exfoliated composites. According to Vaia et al.,¹⁴ the degree of exfoliation can be improved through the aid of conventional shear devices such as extruders, mixers, ultrasonicators, etc.

In this article, ultrasonicator was used as a means of applying external shearing forces to enhance better

Correspondence to: A. Boukerrou (aboukerrou@yahoo.fr).

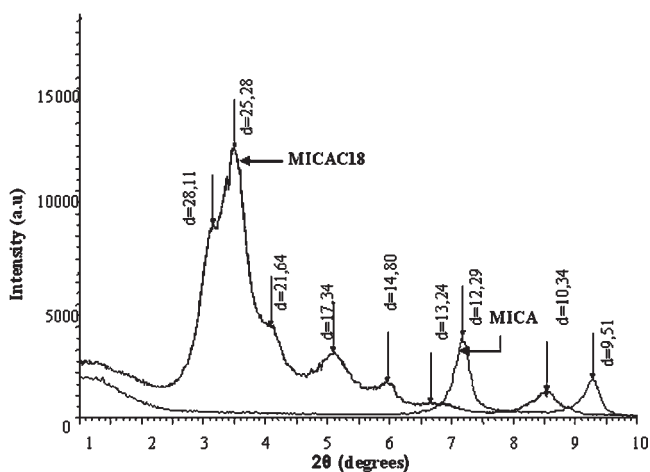


Figure 1 WAXD patterns of unmodified mica (MICA) and modified mica (MICAC18). The distances are given in Å.

dispersion of the silicate clay in the matrix. Initially, the procedure consisted of swelling the clays in a curing agent of low viscosity for better diffusion into the intragalleries. Then, the epoxy prepolymer was added. Under these conditions, it was expected for the occurrence of a better dispersion. The use of the ultrasonic process was to improve the break up of layered silicate bundles and further reduction of the dispersion size with better homogeneity.¹⁵

Therefore, the objective of this work was aimed to prepare nanocomposites based on DGEBA/D2000 modified by MICA clay, using ultrasound-assisted mixing process. Morphology, mechanical, and thermomechanical properties were investigated using wide angle X-ray scattering (WAXS), transmission electron microscopy (TEM), tensile tests, and dynamic mechanical thermal analysis (DMTA) analysis. The results were compared with those of the unmodified nanocomposites and the neat matrix.

EXPERIMENTAL

Materials used

The nanofiller used was a synthetic fluorosilicate called MICA, provided by COOP Chemicals (from Japan), whose trade name is SOMASIF ME100. It was a magnesium silicate containing Na, Al, and F according to the following chemical structure: $\text{Na}_{1.08}\text{Mg}_{1.96}\text{Al}_{0.13}\text{Si}_4\text{O}_{10}\text{F}_2$ and its cation exchange capacity (CEC) is 70 mequiv/100 g.¹ The organic system was based on epoxy/amine; the prepolymer diglycidyl ether of bisphenol A is manufactured by Vantico (Paris, France) under the grade name DGEBA LY 556 having the following characteristics: polymerization degree $n = 0.15$ and $M_n = 382.6$ g/mol. The curing agent is an aliphatic diamine with a polyoxypropylene backbone supplied by Huntsman (Everberg, Belgium)

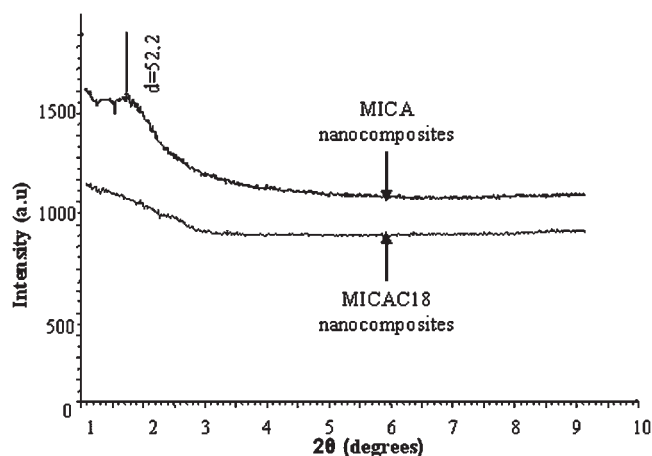


Figure 2 WAXD patterns of DGEBA/D2000/MICA and DGEBA/D2000/MICAC18 nanocomposites. The distance is given in Å.

under the trade name Jeffamine D2000, with $M_n = 1970$ g/mol.

Organoclay preparation

The method of organoclay preparation was similar to that used by Le Pluart et al.¹⁶ The silicates were exchanged with octadecylammonium ions at 80°C with two CEC's amine/clay ratio. About 0.2 mol of octadecylamine was dissolved in 20 L of 0.01 mol/L of hydrochloric acid solution (based on deionized water). The solution was stirred at 80°C for 3 h. Then, 100 g of clay was added to the solution, and the whole mixture was stirred at the same temperature for three more hours. The solution was filtered, and the silicates were further washed more than six times with hot deionized water and once with hot ethanol : water (1 : 1) mixture, so that no chloride was detected upon adding 0.1 mol/L aqueous AgNO_3 .

The resulting organoclay was then dried at 85°C for 36 h and kept dry in a vacuum box. After modification, the organoclay is known as MICAC18.

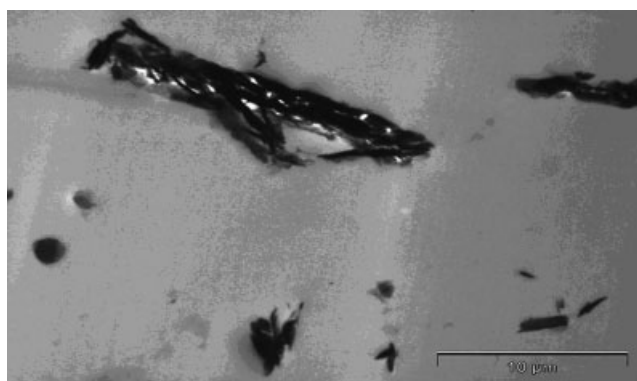


Figure 3 Transmission electronic microscopy (TEM) of DGEBA/D2000/MICA nanocomposites

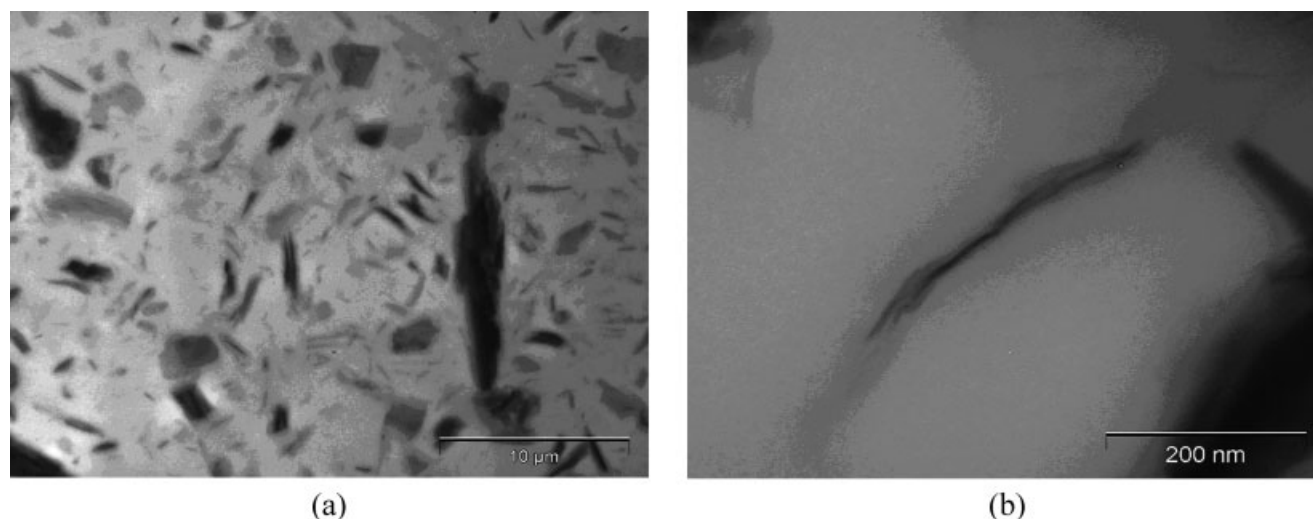


Figure 4 (a) TEM of DGEBA/D2000/MICAC18 nanocomposites. Scale level is 10 μm . (b) TEM of DGEBA/D2000/MICAC18 nanocomposites. Scale level is 200 nm.

Preparation of epoxy-nanocomposites

Silicate clay (5 phr) and the curing agent were initially sonicated at 80°C for 10 min using an ultrasonic processor device at a frequency of 20 kHz and amplitude at 6 μm . The temperature of 80°C corresponds to the first curing temperature of the reactive agents. The epoxy prepolymer was then added to the mixture, and the whole mixture was stirred for more than 15 min. Then, the blend was poured into a steel mold and cured for 2 h at 80°C followed by a postcure during 3 h at 125°C. The stoichiometric mass ratio of DGEBA/D2000 was calculated, and the value was 2.65 according to the diamine functionality which was itself determined by chlorhydric acid in dioxane (3.54).¹⁷

Nanocomposite characterization

Wide angle X-ray scattering

Wide angle X-ray scattering (WAXS) measurements were performed at room temperature on a SIEMENS

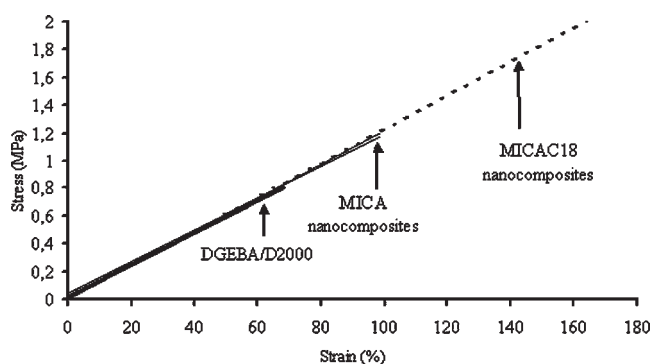


Figure 5 True stress-strain parameters of DGEBA/D2000 matrix, MICA, and MICAC18 nanocomposites.

D500 diffractometer (Germany) with a Brentano Bragg geometry goniometer with Cu K α radiation ($\lambda = 1.54 \text{ \AA}$), operating at 40 kV and 30 mA. The diffraction patterns were collected between angles 2θ of 1°–10°, at a scanning rate and step size of 5°/min and 0.02°, respectively.

Transmission electron microscopy

The different nanocomposite samples were ultramicrotomed with a diamond knife on a Leica Ultracut UCT microtome (Bannock-burn IL) at -70°C , to give sections with a nominal thickness of 70 nm. The sections were transferred from dry conditions (-70°C) to carbon-coated 200-mesh Cu grids. The TEM images were obtained at 120 kV under low-dose conditions, with a Philips CM120 electron microscope (Netherlands).

Tensile testing

The stress-strain parameters were measured according to NF T 51-034 method on a tensile machine 2/M from MTS Society (Toulouse, France). The specimen has the shape H3 with the following dimensions: $2 \times 4 \times 10 \text{ mm}^3$, while the measurements were carried out at room temperature with a crosshead speed of 5 mm/min. An average value with five samples was determined.

The theory of rubber elasticity¹⁸ was used to relate the deformation state at the molecular level to the externally applied deformation. In the case of uniaxial deformation, the true stress (force divided by the deformed area) is defined for dry networks formed in the bulk state as

TABLE I
Mechanical Properties at 25°C of the Nanocomposites Based on the DGEBA/D2000 Matrix

Matrix DGEBA/D2000	G (MPa)	G/G ₀	σ _r (MPa)	ε _r (%)	W _b (10 ⁻³ J)	W _b /W ₀
Unloaded	0.56	1	0.8 ± 0.048	69 ± 5	26 ± 3	1
MICA (5 phr)	0.64	1.14	1.10 ± 0.05	96 ± 3	50 ± 4	1.92
MICAC18 (5 phr)	1.26	2.25	1.99 ± 0.07	153 ± 3	118 ± 2	4.54

G₀, elastic modulus of the neat matrix; ε_r, elongation at break; W₀, energy at break of the neat matrix; W_b, energy at break of the nanocomposite; σ_r, stress at break.

$$\sigma = (\rho RT/M_c)(\lambda^2 - \lambda^{-1})$$

where σ is the true stress, ρ the network density, R = kN_a (where k is the Boltzmann constant and N_a is the Avogadro number), T the absolute temperature, M_c the average molecular weight between crosslinks, and λ is the extension ratio defined as the ratio of the final length of the sample in the direction of stretch to the initial length before deformation.

Dynamic mechanical thermal analysis

The DMTA of the nanocomposite properties were determined by using a Rheometrics Dynamic Analyzer (Paris, France). The tests were carried out in the torsion deformation mode at a frequency of 1 Hz, with a temperature program ranging from -100°C to 50°C at a heating rate of 3°C/min under a controlled strain of 0.17% corresponding to the linear portion of the viscoelastic domain of the material.

RESULTS AND DISCUSSION

Morphology

Figure 1 shows the XRD patterns for both MICA and MICAC18, respectively, in the 2θ region of 1°–10°. It is observed by the formation of a peak at almost 2θ = 7.3° corresponding to a d-spacing of 12.3 Å for MICA, which is assigned to the [001] lattice spacing of the unmodified clay. After MICA modification with octadecylammonium ions, the initial d-spacing increases from 12.3 to 28.1 Å. The swelling of the gallery layers is generally interpreted as a result of the organic modification of the MICA involving cationic exchange between ions of the MICA and those of alkyl ammonium.¹⁹

Figure 2 exhibits the XRD patterns of DGEBA/D2000/MICA and DGEBA/D2000/MICAC18 nanocomposites. It is noted that the [001] diffraction peak of the DGEBA/D2000/MICA nanocomposites appears at 2θ = 1.6°, with basal spacing of 52.2 Å. This result shows much higher d-spacing compared with unmodified MICA and this is interpreted by intercalation of the MICA by the epoxy/amine precursors. On the contrary, no peak is observed in the diffraction pattern of the organoclay. This result indicates that the MICAC18

has been finely dispersed in the epoxy matrix, suggesting that a great amount of polymer has entered the gallery space, expanding the clay layers so far apart that diffraction cannot be observed with wide angle (2θ > 1°) XRD techniques.

Figures 3 and 4 show the TEM images of MICA and MICAC18 nanocomposites, respectively. In Figure 3, it is observed that the formation of agglomerates indicate clearly the poor dispersion of the clays in the epoxy matrix, because of the poor interactions between a polar unmodified mica and the organic matrix. In contrast, Fig. 4(a,b) illustrates a better dispersion of the clay particles and layers in the matrix resulting from the swelling of the MICAC18 in the nanocomposites, indicating a good compatibility between organophilic modified mica and organic matrix.

Mechanical properties

Figure 5 shows the stress–strain curves relative to the neat epoxy matrix, MICA, and MICAC18 nanocomposites. In this figure, an increase of both the stress and the strain at break is observed in both nanocomposite samples compared with the epoxy matrix. In fact, the stress at break increases by 38% for MICA and 150% for MICAC18. Similar behavior is also noted in the case of strain at break, where an increase of 40% and 120% is found for both unmodified and modified MICA nanocomposites, respectively, (Table I). The increase of these two parameters could be attributed to better dispersion of organophilic clay in the nanocomposites.^{20,21} These results are in agreement with those obtained by TEM.

Figure 6 shows the curves of the true stress as a function of (λ² - λ⁻¹) for the epoxy matrix, MICA, and MICAC 18 nanocomposites. The general shape of the curves fits well a linear relationship that is described by the following equation: σ = G (λ² - λ⁻¹), where G represents the slope of the curve defined as a rubber elasticity modulus.¹⁸ In both samples, the stiffness is improved; however, it is more pronounced for the MICAC18 samples. Indeed, this characteristic is improved by 14% and 125% for MICA and MICAC18 nanocomposites, respectively. This result is consistent with the data reported by Pinnavaia et al.²² and Wang and Pinnavaia,²³ who indicated that the addition of 5 wt % of particulate nanofillers in epoxy amine

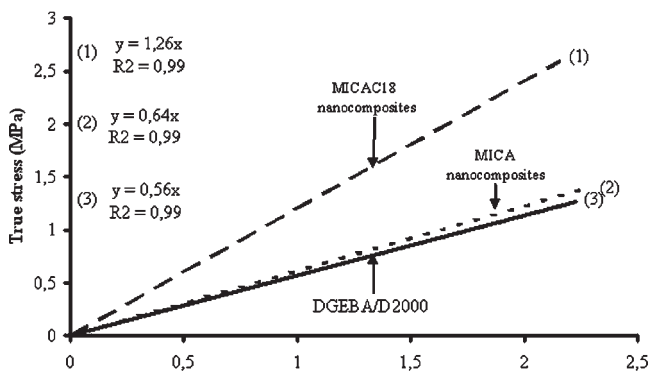


Figure 6 True stress as function of $(\lambda^2 - \lambda^{-1})$ of DGEBA/D2000 matrix, MICA, and MICAC18 nanocomposites.

network leads to an increase by twice of the rubber elasticity of the nanocomposites compared with that of the matrix. The G values are also reported in detail in Table I. When the dispersion of organoclays in the matrix DGEBA/D2000 is carried out manually, the mechanical properties do not increase significantly,²¹ compared with the results obtained with ultrasound mixing process. The improvement of mechanical properties might be linked to the state of dispersion at the micron and the nanometer scale level.²¹

Dynamic thermal mechanical properties

The dynamic mechanical properties of MICA and MICAC18 nanocomposites were studied over a wide range temperature: -100°C to 50°C . The variation of $\tan \delta$ as a function of temperature for both nanocomposites is shown in Figure 7. In this figure, it is observed that one relaxation peak corresponding to the mechanical transition temperature slightly decreases in the presence of organoclay. According to the literature,²⁴ this behavior is attributed to a reduction of the polymer volume fraction due to presence of the filler. This means that, at low temperature, the

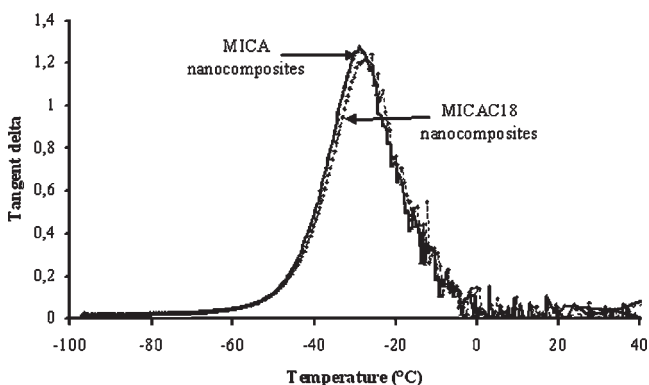


Figure 7 $\tan \delta$ as a function of temperature for MICA and MICAC18 nanocomposites.

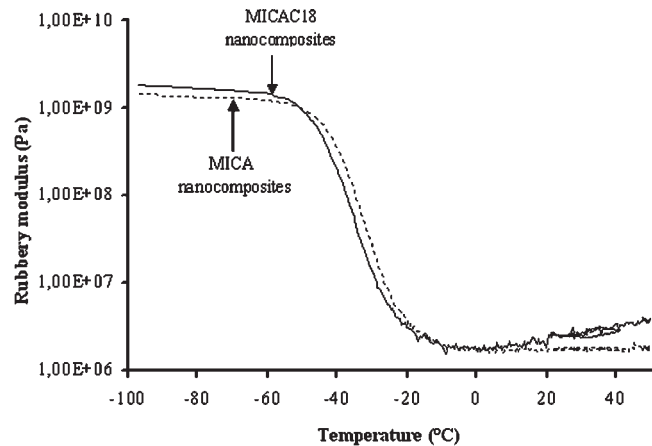


Figure 8 Storage modulus as a function of temperature for DGEBA/D2000 matrix, MICA, and MICAC18 nanocomposites measured at 1 Hz.

polymer matrix by itself is responsible for a high proportion of energy dissipation, while the nanoparticles strongly absorb any energy.

Figure 8 shows the storage modulus (elastic modulus) of MICA and MICAC18 nanocomposites as a function of temperature. It is noted that the organoclay induces a slight increase in modulus. All the data are given in detail in Table II.

CONCLUSIONS

From this study, the following conclusions can be drawn. The modification of MICA surface by octadecylammonium ions leads to an intercalation as revealed by WAXS analysis. The addition of 5 phr of MICAC18 to the matrix and the use of ultrasound-assisted mixing process result in better dispersion of the nanofiller. As a result, an improvement in both the stress-strain parameters at break and the viscoelastic properties is obtained. Finally, the MICAC18 increases considerably both the stiffness and the energy at break of the nanocomposites, even though it is not easy to obtain a compromise between the two parameters. In our case, the homogeneity of the morphology induces a significant increase of both the stiffness and the

TABLE II
Values of the Storage Modulus (G'), Mechanical Transition Temperature (T_m), and $\tan \delta$ of Various Samples Based on DGEBA/D2000 Matrix, MICA, and MICAC18 Nanocomposites Recorded at 1 Hz

Formulation codes	Elastic modulus (G') at 25°C (GPa)	T_m ($^\circ\text{C}$)	$\tan \delta$
DGEBA/D2000	1.43	-31	1.26
MICA/DGEBA/D2000	1.82	-29	1.24
MICAC18/DGEBA/D2000	1.94	-27	1.22

energy at break by roughly 125% and by more than 350% respectively.

References

1. Boukerrou, A.; Duchet, J.; Fellahi, S.; Sautereau, H. *J Appl Polym Sci* 2006, 102, 1380.
2. Isik, I.; Yilmazer, U.; Bayram, G. *Polymer* 2003, 44, 6371.
3. Kornman, X.; Lindberg, H.; Berglund, L. A. *Polymer* 2001, 42, 4493.
4. Chin, I. J.; Thurn-Albrecht, T.; Kim, H. C.; Russel, T. P.; Wang, J. *Polymer* 2001, 42, 5947.
5. Evora, V. M. F.; Shukla, A.; *Mater Sci Eng A* 2003, 363, 358.
6. Kornman, X.; Lindberg, H.; Berglund, R. A. *Polymer* 2001, 42, 1303.
7. Nigam, V.; Setua, D. K.; Matur, G. N.; Kar, K. K. *J Appl Polym Sci* 2004, 93, 2201.
8. Mascia, L.; Prezzi, I. *Adv Polym Tech* 2005, 24, 91.
9. Mascia, L.; Prezzi, I.; La Vormia, M. *Polym Eng Sci* 2005, 45, 1039.
10. Kinloch, A. J.; Lee, J. H.; Taylor, A. C.; Sprenger, S.; Eger, C.; Egan, D. *J Adhes* 2000, 79, 867.
11. Alexandre, M.; Dubois, P. *Mater Sci Eng* 2000, 28, 1.
12. Park, J.; Jana, S. C. *Macromolecules* 2003, 36, 6391.
13. Asma, Y.; Jandro, L. A.; Issac, M. D. *Scripta Mater* 2003, 40, 81.
14. Vaia, R. A.; Jandt, K. D.; Kramer, E. J.; Giannelis, E. P. *Chem Mater* 1996, 8, 2628.
15. Ryu, J. G.; Kim, H.; Lee, J. W. *Polym Eng Sci* 2004, 44, 1198.
16. Le Pluart, L.; Duchet, J.; Sautereau, H.; Gerard, J. F. *Macromol Symp* 2003, 194, 155.
17. Lan, T.; Pinavaia, T. J. *Chem Mater* 1994, 6, 2216.
18. Bokobza, L. *Macromol Symp* 2001, 171, 163.
19. Le Pluart, L.; Duchet, J.; Sautereau, H. Gerard, J. F. *J Adhes* 2002, 78, 645.
20. Lee, K. Y.; Goettler, L. A. *Polym Eng Sci* 2004, 44, 1103.
21. Le Pluart, L.; Duchet, J.; Sautereau, H. *Polymer* 2005, 46, 12267.
22. Pinnavaia, T. J.; Lan, T.; Karavatina, P. D.; Wang, Z.; Shi, H. *ACS Polym Mater Sci Eng* 1996, 74, 117.
23. Wang, Z.; Pinnavaia, T. J. *Chem Mater* 1998, 10, 1820.
24. Wang, M. J. *Rubber Chem Technol* 1998, 71, 520.